Cancellation costs for leading backreaction in a tachyonic spectator portal

Abstract

An initially unspecified spectator state need not produce a unique background response, even when its canonical linear transfer is fixed. We construct two retarded, quadratic response kernels for a canonical spectator on a specified noncanonical two-field background: the leading scalar displacement and the leading isotropic change in the logarithmic scale factor. We minimize the former over all one-mode quantum second moments while constraining the latter. Established covariance minimization gives an explicit, attained cancellation frontier when the displacement kernel is positive definite and the expansion kernel is indefinite. In a fixed early-time portal benchmark these conditions hold, and requiring zero final expansion response increases the minimum displacement by a factor of approximately 1.3391. Omitting the direct spectator stress changes the expansion kernel to positive definite, removing the cancellation possibility despite a small change in the displacement kernel. The result concerns a finite canonically normalized mode and the leading scalar projection of its response. It neither selects a cosmological state nor supplies a renormalized continuum prediction or a uniform nonlinear-validity bound.

1 Question and relation to established results

Tachyonic amplification and hybrid exits are established mechanisms [1–3]. A large growth integral is not by itself a normalized mode solution, and a mode transfer is not an initial state. The distinction between the rescaled mode, its Wronskian, the growth exponent and matching is explicit in Ref. [3]. Here we ask a subsequent question: can an allowed initial covariance hide a leading expansion response, and what field response must remain when it does?

The mathematical ingredients have substantial prior art. Positive quadratic covariance minima follow from symplectic trace minimization [4, 5]; an explicit all-input-state quadratic-energy minimum after a Gaussian channel appears in Ref. [6, Theorem 19]. Optimizing one state over a time-smeared cosmological energy is also established [7]. Semidefinite alternatives underlying cancellation and nonattainment are standard [8]. We do not claim these tools, a general quantum energy inequality, or a new portal operator. In particular, a radial-squared cosine portal occurs in Ref. [9, eq. (2.7), arXiv v2].

Phase cancellation of a spectrum contribution while excited-state energy remains constrained is also familiar in a different, slow-roll continuum setting [10, sections 3.2.1 and 5.2]. Thus the general cancellation-versus-backreaction observation is not a new mechanism.

Our contribution is a conditional response calculation and its sharp tradeoff: the actual retarded scalar kernels of a specified portal background, including the direct Friedmann source, admit cancellation of one endpoint response while enforcing a larger minimum of another. The analytic frontier makes the constraint precise and displays its attaining covariance. Unlike vacuum-initialized amplification or energy-exchange calculations [11, 12], the comparison is over all finite one-mode second moments satisfying the canonical uncertainty relation. This is not an assertion that the optimizing state was physically prepared.

2 Declared portal and finite-mode response

2.1 Action and background

Use signature $(-,+,+,+)$, reduced Planck mass $M_{\rm Pl}$ and $X=-(\partial\theta)^2/2$. The declared action is

$$S=\int \mathrm{d}^4x\sqrt{-g}\left[\frac{M_{\rm Pl}^2R}{2}-\frac{(\partial\sigma)^2}{2}+P(X,z,\theta)-\frac{(\partial\chi)^2}{2}-\frac{M^2(\sigma,\theta)\chi^2}{2}\right],\quad z=\frac{\sigma}{f_\sigma},\tag{1}$$

where

$$P=X+\frac{5(z-2/\sqrt{3})^2X^2}{3\Lambda^4}-E_cF\left(z,b_*+\beta\theta/M_{\rm Pl}-5X/\Lambda^4\right)-V_s(\theta),\tag{2}$$

$$F(z,b)=\frac{z^4}{4}-\frac{z^2}{2}+bz,\qquad M^2=m_0^2+2\lambda(v+\sigma)^2\cos(2\theta/f).\tag{3}$$

The quartic V_s, parameters and input trajectory are specified in Appendix A. The canonical χ action is an explicit completion of an earlier mass diagnostic, not a uniquely recovered historical action. It is local near $\chi=0$; when $M^2<0$, the purely quadratic χ potential is not a globally stable nonlinear completion.

At $\bar\chi=0$, the flat-FLRW background obeys

$$\rho_b=\dot\sigma^2/2+2XP_X-P,\qquad H^2=\rho_b/(3M_{\rm Pl}^2),\tag{4}$$

$$\ddot\sigma+3H\dot\sigma-P_\sigma=0,\qquad K\ddot\theta+3HP_X\dot\theta+P_{X\sigma}\dot\sigma\dot\theta-P_\theta=0,\tag{5}$$

with $K=P_X+2XP_{XX}$ and $P_{X\theta}=0$ for this P. The benchmark uses $H_*\simeq 2.020972936\times10^{-6}$ as a model input in $M_{\rm Pl}=1$ units; it is not redetermined from a primordial amplitude. Its background exit occurs in the σ/θ system. No χ-driven exit is inferred.

2.2 Canonical mode and normalization

At $\bar\chi=\dot{\bar\chi}=0$, $\delta\chi$ is gauge invariant and its stress starts at quadratic order. The mixed terms $\delta\sigma(\delta\chi)^2$, $\delta\theta(\delta\chi)^2$ and $\delta g(\delta\chi)^2$ are cubic, so its linear block decouples without a subhorizon assumption. For $q=a^{3/2}\delta\chi_k$,

$$\ddot q+\Omega^2q=0,\qquad \Omega^2=k_{\rm com}^2/a^2+M^2-\frac{9}{4}H^2-\frac{3}{2}\dot H.\tag{6}$$

Additional Z_2-even derivative or curvature portals could preserve decoupling while changing this equation; they are not included here.

Take a real eigenfunction e_k in a compatible periodic comoving box of volume V, with $\int_V e_k^2\mathrm{d}^3x=1$. Set

$$\chi(\tau,\vec x)=\frac{a^{-3/2}}{\sqrt{H_*}}Q(\tau)e_k(\vec x),\quad \tau=H_*t,\quad Z=(Q,P_Q)^T,\quad P_Q=Q',\quad [Q,P_Q]=i\hbar.\tag{7}$$

The real transfer satisfies $Z(\tau)=T(\tau)Z_i$, $T_i=I$, $\det T=1$. The initial uncentered symmetrized second moment is $C_{ab}=\langle\{Z_{i,a},Z_{i,b}\}\rangle/2$. Every state with finite moments satisfies

$$C\succ 0,\qquad \det C\geq\nu^2,\qquad \nu=\hbar/2>0.\tag{8}$$

Conversely every matrix in (8) has a centered Gaussian representative. Thus minimizing a quadratic functional over this cone does not assume that all states are Gaussian. Volume enters through the explicit factor $\gamma=(VH_*^3)^{-1}$; no observed volume or cosmological vacuum is assigned.

2.3 Retarded scalar kernels

Use normalized background coordinates

$$x = (\sigma/f_\sigma, \dot\sigma/(f_\sigma H_*), \theta/M_{\rm Pl}, \dot\theta/(M_{\rm Pl}H_*), N), \quad N = \ln a, \tag{9}$$

and write their unperturbed proper-time equations as $x' = \mathcal{F}(x)$. With $h = H/H_*$, let

$$E = T^T e_1 e_1^T T, \qquad D = T^T r r^T T, \qquad r = (-3h/2, 1)^T, \tag{10}$$

$$W_b = (k_{\rm com}^2/a^2 + M^2)/H_*^2, \qquad L_h = \frac{H_*^2 a^{-3}}{12 M_{\rm Pl}^2 h}(D + W_b E). \tag{11}$$

The spatially averaged moment and direct Friedmann correction are

$$\langle \chi^2 \rangle_V = \gamma H_*^2 a^{-3} \operatorname{tr}(EC), \qquad \delta h_\chi = \gamma \operatorname{tr}(L_h C). \tag{12}$$

The matrix-valued sources for the leading scalar response are

$$\mathcal{S}_1 = \mathcal{S}_3 = 0, \qquad \mathcal{S}_5 = L_h, \tag{13}$$

$$\mathcal{S}_2 = -\frac{a^{-3} M_{,\sigma}^2}{2 f_\sigma} E - 3 x_2 L_h, \tag{14}$$

$$\mathcal{S}_4 = -\frac{a^{-3} M_{,\theta}^2}{2 K M_{\rm Pl}} E - 3 (P_X/K) x_4 L_h. \tag{15}$$

Let $\mathcal{R}_i$ solve

$$\mathcal{R}_i' = \sum_j \frac{\partial \mathcal{F}_i}{\partial x_j} \mathcal{R}_j + \mathcal{S}_i, \qquad \mathcal{R}_i(\tau_i) = 0. \tag{16}$$

Then the order-χ^2 response is $\delta x_i^{(2)} = \gamma \operatorname{tr}(\mathcal{R}_i C)$. The initial homogeneous coordinates match the reference solution, while H satisfies the Friedmann constraint with the additional spectator stress. In particular, its initial correction is not separately set to zero.

These are the homogeneous scalar/isotropic projections in a fixed proper-time convention. A real spatial mode also has anisotropic stress and can source shear. Its shear energy enters the scalar Friedmann constraint at higher order, so it does not change (13)–(15); the complete metric response is not being computed. The signed kernel for N must not be replaced by a positive energy norm.

3 An attained cancellation frontier

Fix an endpoint and write

$$B = \mathcal{R}_1(\tau_f), \qquad A = \mathcal{R}_5(\tau_f), \qquad \delta z^{(2)} = \gamma \operatorname{tr}(BC), \quad \delta N^{(2)} = \gamma \operatorname{tr}(AC). \tag{17}$$

Suppose $B \succ 0$ and A is indefinite. The unconstrained displacement floor is the established covariance minimum $2\nu\sqrt{\det B}$. We now constrain the different, signed response.

Proposition 1 (Cancellation cost)**.** *Let $B \succ 0$, $\det A < 0$ and $\nu > 0$. Define*

$$b = \det B, \quad d = -\det A, \quad c = \operatorname{tr}(\operatorname{adj}(B) A), \quad q = b + \frac{c^2}{4d}, \quad \epsilon_c = \frac{\nu |c|}{\sqrt{b}}. \tag{18}$$

For $\epsilon \geq 0$, the minimum

$$F(\epsilon) = \min_{C \succ 0,\, \det C \geq \nu^2,\, |\operatorname{tr}(AC)| \leq \epsilon} \operatorname{tr}(BC) \tag{19}$$

is attained uniquely, at $\det C = \nu^2$*, and equals*

$$F(\epsilon) = \begin{cases} \sqrt{q}\sqrt{4\nu^2 + \epsilon^2/d} - \dfrac{\epsilon|c|}{2d}, & 0 \le \epsilon < \epsilon_c, \\ 2\nu\sqrt{b}, & \epsilon \ge \epsilon_c. \end{cases} \tag{20}$$

For $c = 0$*, the second branch applies at every* $\epsilon \ge 0$*.*

Proof. For any real λ with $D_\lambda = B + \lambda A \succ 0$, the known positive trace minimum gives

$$\operatorname{tr}(BC) \ge 2\nu\sqrt{\det D_\lambda} - |\lambda|\epsilon, \qquad \det D_\lambda = b + c\lambda - d\lambda^2. \tag{21}$$

The connected interval of positive determinant containing zero has positive-definite D_λ. For $0 \le \epsilon < \epsilon_c$ and $c \ne 0$, maximize (21) at

$$\lambda_\epsilon = \operatorname{sgn}(c)\left[\frac{|c|}{2d} - \frac{\epsilon\sqrt{q}}{\sqrt{d}\sqrt{4\nu^2 d + \epsilon^2}}\right]. \tag{22}$$

The positive-trace optimizer

$$C_\epsilon = \nu\sqrt{\det D_{\lambda_\epsilon}}\, D_{\lambda_\epsilon}^{-1} \tag{23}$$

obeys $\operatorname{tr}(AC_\epsilon) = \operatorname{sgn}(c)\epsilon$ and attains (20). At larger tolerance the unrestricted optimizer $C_{\text{free}} = \nu\sqrt{b}B^{-1}$ is feasible. Equality in the positive trace minimum proves uniqueness, including the exact-cancellation endpoint without appealing to an interior-feasibility assumption there. □

Exact cancellation costs

$$\frac{F(0)}{F(\infty)} = \sqrt{1 + \frac{c^2}{4bd}}. \tag{24}$$

For a physical tolerance ϵ_N in the stated scalar projection, $\delta z^{(2)} \ge \gamma F(\epsilon_N/\gamma)$. The ratio (24) is independent of V and of canonical-coordinate changes applied consistently to both kernels and the covariance. This is an observable-response tradeoff in the declared model, not a transfer singular value. The proof uses established covariance optimization; the application below supplies the retarded matrices and their physical distinction.

4 Fixed-background benchmark

4.1 Input and numerical response

The background is a stored numerical solution of (5), with $a(0) = 1$. We use one existing original trajectory and one independently stored DOP853 control, retaining a small input segment in the reproduction material. We do not repeat the historical background parameter suite. The momentum and interval are fixed before the response calculation:

$$k_{\text{com}} = 4.4118807290472784 \times 10^{-8}, \quad \tau_i = 0.023091159471767778, \quad \tau_f = 0.30. \tag{25}$$

This early interval is chosen to resolve a finite response with manageable conditioning; it is not a certified endpoint of physical linearity. The mode becomes tachyonic inside it. The quoted momentum is the historical low endpoint $0.05H_{\text{exit}}$ converted to comoving units. Its physical momentum stays far below Λ on this segment. No continuum momentum integral or state spectrum is inferred.

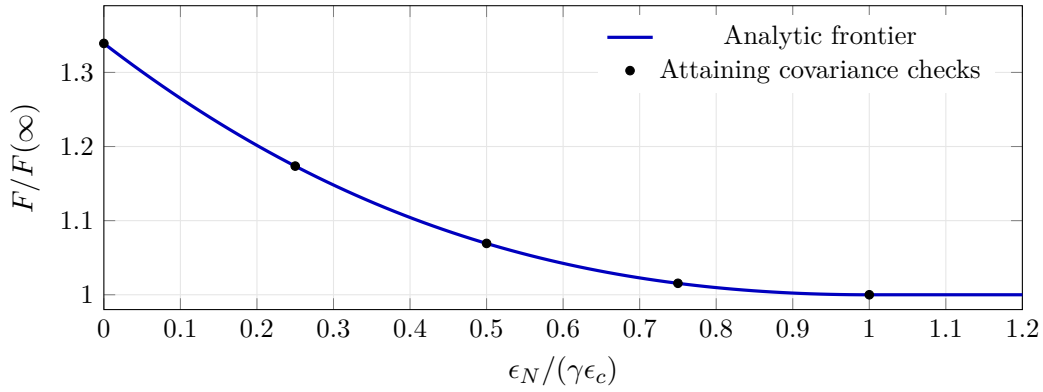


Figure 1: Minimum leading displacement as the allowed magnitude of the final scalar expansion response increases. The horizontal coordinate uses the crossover ϵ_c of the covariance problem. Both actual responses scale with the explicit volume factor γ; the ratio shown does not. The endpoints compare exact final expansion cancellation with the unconstrained displacement minimum. Numerical checks are from the finite benchmark, not measured cosmological states.

With $\hbar = 1$, the response matrices per unit γ are approximately

$$B = \begin{pmatrix} 1.35645111885 \times 10^{-5} & 3.63201448919 \times 10^{-6} \\ 3.63201448919 \times 10^{-6} & 9.77242570977 \times 10^{-7} \end{pmatrix}, \tag{26}$$

$$A = \begin{pmatrix} -3.46650724056 \times 10^{-9} & -9.55264201270 \times 10^{-10} \\ -9.55264201270 \times 10^{-10} & -2.56870942652 \times 10^{-10} \end{pmatrix}. \tag{27}$$

Their eigenvalues are $(4.42231 \times 10^{-9}, 1.45373 \times 10^{-5})$ and $(-3.72930 \times 10^{-9}, 5.92195 \times 10^{-12})$, respectively. Thus a positive field response coexists with a cancelable signed expansion response.

The unconstrained displacement floor is $2.53551845 \times 10^{-7}\gamma$. Exact cancellation of $\delta N^{(2)}$ raises it to $3.39537687 \times 10^{-7}\gamma$, a factor 1.33912529. The crossover expansion tolerance is $1.32358761 \times 10^{-10}\gamma$. A mathematical attaining covariance for zero final expansion is

$$C_* \simeq \begin{pmatrix} 0.8642676502 & -3.2108367736 \\ -3.2108367736 & 12.2178271793 \end{pmatrix}, \qquad \det C_* = \frac{1}{4}. \tag{28}$$

It is not an inferred initial state. Earlier values of $\delta N^{(2)}/\gamma$ for this same C_* are approximately 1.58×10^{-11}, 3.79×10^{-11} and 5.34×10^{-11} at $\tau = 0.0731, 0.15, 0.2118899$. The endpoint cancellation is not a cancellation of the whole history. Indeed, a single early positive-definite N kernel already prevents that stronger claim.

4.2 The direct gravitational source is qualitatively relevant

For diagnosis only, omit L_h from all direct sources in (13)–(15), retaining the background Jacobian. This is not a consistent alternative physical model. The displacement kernel changes relatively by only 2.40×10^{-5}, but the N kernel becomes positive definite, with eigenvalues approximately $(4.70 \times 10^{-12}, 1.70 \times 10^{-8})$. Exact expansion cancellation would then be impossible for any covariance satisfying (8). A term that is small in one response channel therefore cannot be discarded when deciding cancelability in another. The effect concerns the scalar retarded response, not a claim of large gravitational energy production.

4.3 Checks and precision

The response ODE evolves T, the five symmetric $\mathcal{R}_i$ and a positive moment Gramian on the fixed background segment. A complex-step Jacobian of the exact background RHS is checked against centered finite differences. Tightening solver settings, halving the interpolation point density and using the stored DOP853 background all preserve the kernel signatures. The largest relative response-matrix change in the interpolation comparison is about 2.63×10^{-11}; the stored-background comparison is below 10^{-12} at the endpoint. Whitening and dual evaluation of the constrained optimizer agree to roughly 10^{-14} relatively.

An additional short finite-amplitude directional check uses the scalar-projected coupled equations. Three deterministic classical directions verify the quadratic map; they are not quantum covariance choices. At amplitudes 0.04 and 0.02, the largest relative discrepancies are approximately 9.8×10^{-7} for the displacement coefficient and 1.6×10^{-3} for the much smaller N coefficient. The latter difference quotients reach a subtraction floor; decreasing the amplitude does not monotonically improve them. These checks substantiate the source factors and leading map, not a nonlinear completion.

All numerical differences are empirical controls, not outward-rounded enclosures of the exact background. The many digits in the data files provide reproducibility, not a matching physical accuracy. Appendix C separates matrix-error assumptions from what these checks establish. One preregistered postprocessing attempt failed by applying the indefinite-kernel formula to a diagnostic case that was positive definite; the corrected run preserves the raw kernels and guards their inertia. The failed attempt is retained in the resource and reproduction records.

5 Scope of the inference

A positive lower bound on a specified leading response does not by itself locate a nonlinear breakdown time. For example, random initial amplitudes that equal $\pm L$ with probability $s/(2L^2)$ each and vanish otherwise have fixed second moment s and fourth moment $sL^2 \to \infty$. A second-moment or quadratic-energy condition therefore cannot uniformly control higher-order remainders for arbitrary ensembles. The present minimization is complete at the stated quadratic order; a nonlinear bootstrap needs additional information about higher moments, support or a justified closure.

The finite canonical mode avoids a UV subtraction problem within its declared domain, but does not supply renormalized continuum stress, a Hadamard state or a complete field spectrum. The choice of V must respect the mode's periodic geometry and remains symbolic. The scalar projection omits induced inhomogeneous and shear dynamics. A full physical interpretation would also require the missing nonlinear portal completion and a controlled expansion over the claimed state class.

The application establishes a sharp, state-dependent cancellation cost within this scope. It illustrates why a small or vanishing net expansion response need not imply absence of a field response, and why omitting direct gravitational sources can change that conclusion. Neither the standard covariance tools nor this one benchmark imply a universal statement about all tachyonic portals. The background scale is an input, and no primordial-spectrum, reheating or gravitational-wave prediction is made.

A Complete benchmark specification

All numerical values below use $M_{\rm Pl} = 1$. The background inputs are

$$H_* = 2.0209729355762865 \times 10^{-6}, \qquad \Lambda = 0.0023, \tag{29}$$

$$f_\sigma = 0.025, \qquad E_c = 0.04(3H_*^2), \tag{30}$$

$$b_* = 0.35, \qquad \beta = -0.0478, \tag{31}$$

and the portal inputs are

$$\lambda = 1.6740193604000272 \times 10^{-5}, \qquad v = 0.03272387838931097, \tag{32}$$

$$f = 0.8549468502440697, \qquad m_0 = 9.817951142008693 \times 10^{-5}. \tag{33}$$

These are declared benchmark parameters, not estimates from observations.

For completeness, the global quartic $V_s(\theta) = \sum_{j=0}^{4} c_j \theta^j$ is fixed algebraically. Let z_+ be the largest real root of $z^3 - z + b_* = 0$, $b_s = 2/(3\sqrt{3})$, $b_R = b_s + 0.001$, $\theta_R = (b_R - b_*)/\beta$, and z_R the negative real root at b_R. Define $A_{\rm eff} = 0.00686$, $B_{\rm eff} = -0.0174$ and

$$c_0 = 3H_*^2 - E_c F(z_+, b_*), \tag{34}$$

$$c_1 = 3H_*^2 A_{\rm eff} - E_c z_+ \beta, \tag{35}$$

$$c_2 = \frac{1}{2}\left(3H_*^2 B_{\rm eff} + \frac{E_c \beta^2}{3z_+^2 - 1}\right), \tag{36}$$

$$u_0 = -E_c F(z_R, b_R) - (c_0 + c_1\theta_R + c_2\theta_R^2), \tag{37}$$

$$u_1 = -E_c z_R \beta - (c_1 + 2c_2\theta_R), \tag{38}$$

$$c_3 = (4u_0 - \theta_R u_1)/\theta_R^3, \qquad c_4 = (\theta_R u_1 - 3u_0)/\theta_R^4. \tag{39}$$

The symbols u_0, u_1 in these equations are residual interpolation conditions, unrelated to ν. This specifies the quartic used by the stored background; no local quadratic potential is substituted for it.

The finite response problem takes the stored background segment as its numerical input. The supplied NPZ files contain exact contiguous slices of the original and DOP853 trajectories, indices 50–895 inclusive, with 846 stored rows spanning $\tau \in [0.01714334695, 0.30686591045]$. The fields are time, $(\sigma, \dot\sigma, \theta, \dot\theta, a)$, N, ρ, P_X, K and ϵ_H. No values were re-fitted when extracting these files. The original-array and slice hashes, together with the source archive hash, are recorded in `reproduction/data/PROVENANCE.json`. The claimed computation is reproducible from these slices; regeneration of the historical full trajectory is not required for the conditional result.

B Source and optimization details

Spatial averaging gives

$$\rho_\chi = \frac{\gamma H_*^4 a^{-3}}{2} \operatorname{tr}[(D + W_b E)C]. \tag{40}$$

Differentiating the expanding Friedmann branch at fixed homogeneous coordinates gives $\delta h_\chi = \rho_\chi/(6M_{\rm Pl}^2 H_*^2 h)$ and hence L_h in (11). The scalar force corrections are $-M_{,\sigma}^2\langle\chi^2\rangle_V/2$ and $-M_{,\theta}^2\langle\chi^2\rangle_V/2$. Normalizing the acceleration equations gives the first terms of (13)–(15); the changes in Hubble friction give the remaining terms. The derivatives are

$$M_{,\sigma}^2 = 4\lambda(v+\sigma)\cos(2\theta/f), \qquad M_{,\theta}^2 = -\frac{4\lambda(v+\sigma)^2}{f}\sin(2\theta/f). \tag{41}$$

The initial value $\mathcal{R}_i = 0$ therefore matches the coordinates rather than the constrained Hubble rate. Corrections to the linear mode transfer due to the induced background begin beyond the order retained here.

For a positive matrix G, set $Y = G^{1/2}CG^{1/2}$. Then

$$\operatorname{tr}(GC) = \operatorname{tr} Y \geq 2\sqrt{\det Y} \geq 2\nu\sqrt{\det G}. \tag{42}$$

Equality holds only for $C = \nu\sqrt{\det G}G^{-1}$. This elementary one-mode case of the established symplectic trace results also shows that the optimizer is pure and centered. In the constrained problem, substituting $G = B + \lambda A$ produces the proof in the main text. The equality covariance is positive definite throughout the active branch, including $\epsilon = 0$, and converges to the unrestricted optimizer at ϵ_c. Thus no infinite squeezing or unattained limiting state is needed for the reported frontier.

Under a canonical change $Z \mapsto SZ$ with $\det S = 1$, the covariance transforms as $C \mapsto SCS^T$ and the kernels as $A \mapsto S^{-T}AS^{-1}$, $B \mapsto S^{-T}BS^{-1}$. The traces and the polynomial $\det(B + \lambda A)$ are invariant. The frontier and its ratio are consequently independent of this basis choice; Euclidean transfer singular values need not share that property.

C Precision, conditional robustness and reproducibility

The baseline retarded system is integrated with DOP853, relative tolerance 3×10^{-12}, absolute tolerance 3×10^{-15} and maximum τ step 0.00035. The comparison calculation uses 2×10^{-10}, 2×10^{-13} and 0.001, respectively. Cubic splines interpolate the fixed background. The code evolves 22 real variables: four transfer entries, fifteen independent response entries and three entries of a positive integrated moment matrix. Symmetric off-diagonal entries contribute twice in traces. The complex-step Jacobian uses step 10^{-25} and is checked at 10^{-20} and against a centered finite difference of step 10^{-6}; the latter relative discrepancy is about 5.83×10^{-11}. The endpoint determinant of the transfer differs from unity by about 3.64×10^{-11}.

An independent exact rational calculation treats the full decimal matrices in the numerical output as exact data. Their determinants establish $B \succ 0$ and $\det A < 0$, and the resulting ratio lies between 1.3391252854672602879 and 1.3391252854672602880. This is a statement about the tabulated decimals, not an enclosure of the exact differential-equation solution.

One explicit sensitivity question can nevertheless be answered rigorously. Suppose the three independent symmetric entries of each matrix vary independently within

$$|\Delta A_{ij}| \leq 10^{-6}\max_{kl}|A_{kl}|, \qquad |\Delta B_{ij}| \leq 10^{-6}\max_{kl}|B_{kl}|. \tag{43}$$

Exact rational interval operations and outward square-root bounds preserve the two kernel signatures and enclose the cancellation ratio in

$$1.33617231400808 \;<\; \frac{F(0)}{F(\infty)} \;<\; 1.34210485596456. \tag{44}$$

The lower displayed decimal is rounded down and the upper one up. This is a hypothetical matrix-data box: the empirical solver, spline and stored-background comparisons do not prove that the exact physical or background error lies in (43). The exact-arithmetic code and its input binding are included separately from the response integrations.

The portable reproduction driver verifies the supplied data hashes, recomputes the nominal response and the direct-source omission diagnostic, evaluates the analytic frontier and its attaining covariances, and compares against the stored reference. Optional controls repeat only the short retarded calculations with the second stored background and half-density interpolation. Python, NumPy and SciPy suffice; the reference environment used Python 3.12.14,

NumPy 2.5.3 and SciPy 1.18.1. Solver tolerances and finite precision imply numerical, rather than byte-for-byte, reproducibility across platforms.

The audit record includes the failed postprocessing attempt as well as its corrected result. Scientific resource records distinguish these short computations from document builds. The source, finite input slices, outputs, exact-data audit and instructions accompany the manuscript. None of these computational checks constitutes an external scientific endorsement or a proof of a renormalized continuum or nonlinear response.

References

[1] A. Linde. Hybrid inflation. *Physical Review D*, 49:748–754, 1994. doi: 10.1103/PhysRevD.49.748. URL https://arxiv.org/abs/astro-ph/9307002v3.

[2] G. Felder, J. García-Bellido, P. B. Greene, L. Kofman, A. Linde, and I. Tkachev. Dynamics of symmetry breaking and tachyonic preheating. *Physical Review Letters*, 87:011601, 2001. doi: 10.1103/PhysRevLett.87.011601. URL https://arxiv.org/abs/hep-ph/0012142.

[3] J.-F. Dufaux, G. N. Felder, L. Kofman, M. Peloso, and D. Podolsky. Preheating with trilinear interactions: Tachyonic resonance. *Journal of Cosmology and Astroparticle Physics*, 2006(07):006, 2006. doi: 10.1088/1475-7516/2006/07/006. URL https://arxiv.org/abs/hep-ph/0602144.

[4] Tohya Hiroshima. Additivity and multiplicativity properties of some Gaussian channels for Gaussian inputs. *Physical Review A*, 73:012330, 2006. doi: 10.1103/PhysRevA.73.012330. URL https://arxiv.org/abs/quant-ph/0511006.

[5] Rajendra Bhatia and Tanvi Jain. On symplectic eigenvalues of positive definite matrices. *Journal of Mathematical Physics*, 56:112201, 2015. doi: 10.1063/1.4935852. URL https://arxiv.org/abs/1803.04647.

[6] Frank Ernesto Quintela Rodriguez, Francesco Anna Mele, Salvatore Francesco Emanuele Oliviero, Vittorio Giovannetti, Ludovico Lami, and Vasco Cavina. Extracting energy via bosonic Gaussian operations, 2025. URL https://arxiv.org/abs/2503.21748.

[7] Heiner Olbermann. States of low energy on Robertson-Walker spacetimes. *Classical and Quantum Gravity*, 24:5011–5030, 2007. doi: 10.1088/0264-9381/24/20/007. URL https://arxiv.org/abs/0704.2986.

[8] Gábor Pataki. On positive duality gaps in semidefinite programming, 2018. URL https://arxiv.org/abs/1812.11796.

[9] G. G. Ross, G. Germán, and J. A. Vázquez. Hybrid natural inflation. *Journal of High Energy Physics*, 2016(05):010, 2016. doi: 10.1007/JHEP05(2016)010. URL https://arxiv.org/abs/1601.03221.

[10] Raphael Flauger, Daniel Green, and Rafael A. Porto. On squeezed limits in single-field inflation - part i, 2013. URL https://arxiv.org/abs/1303.1430v1.

[11] Eemeli Tomberg and Hardi Veermäe. Tachyonic preheating in plateau inflation. *Journal of Cosmology and Astroparticle Physics*, 2021(12):035, 2021. doi: 10.1088/1475-7516/2021/12/035. URL https://arxiv.org/abs/2108.10767.

[12] Ayan Chakraborty and Debaprasad Maity. Squeezing, chaos and thermalization in periodically driven quantum systems: the case of bosonic preheating. *Journal of High Energy Physics*, 2024 (02):110, 2024. doi: 10.1007/JHEP02(2024)110. URL https://arxiv.org/abs/2309.10116.